frontiers in Materials

ORIGINAL RESEARCH
published: 23 November 2020
doi: 10.3389/fmats.2020.594515

Using Poloxamer® 407 as Building Block of Amphiphilic Poly(ether urethane)s: Effect of its Molecular Weight Distribution on Thermo-Sensitive Hydrogel Performances in the Perspective of Their Biomedical Application

Rossella Laurano[1], *Michela Abrami*[2], *Mario Grassi*[2], *Gianluca Ciardelli*[1], *Monica Boffito*[1*†] *and Valeria Chiono*[1†]

[1] *Department of Mechanical and Aerospace Engineering, Politecnico di Torino, Torino, Italy,* [2] *Department of Engineering and Architecture, Università degli Studi di Trieste, Trieste, Italy*

OPEN ACCESS

Edited by:
Miriam Navlani-García, University of Alicante, Spain

Reviewed by:
Mehdi Derradji, Polytechnic School of Algiers, Algeria
Dagmar Merinska, Tomas Bata University in Zlín, Czechia

***Correspondence:**
Monica Boffito
monica.boffito@polito.it

†These authors have contributed equally to the supervision of the first author.

Specialty section:
This article was submitted to Polymeric and Composite Materials, a section of the journal Frontiers in Materials

Received: *14 August 2020*
Accepted: *19 October 2020*
Published: *23 November 2020*

Citation:
Laurano R, Abrami M, Grassi M, Ciardelli G, Boffito M and Chiono V (2020) Using Poloxamer® 407 as Building Block of Amphiphilic Poly(ether urethane)s: Effect of its Molecular Weight Distribution on Thermo-Sensitive Hydrogel Performances in the Perspective of Their Biomedical Application. Front. Mater. 7:594515. doi: 10.3389/fmats.2020.594515

Due to its hydroxyl terminal groups, Poloxamer® 407 (P407), a commercially available poly(ethylene oxide)-poly(propylene oxide)-poly(ethylene oxide) (PEO-PPO-PEO) triblock copolymer can be used as macrodiol for the synthesis of high molecular weight amphiphilic poly(ether urethane)s (PEUs). This work was aimed at studying the effect of P407 purification by removing PEO-PPO diblock copolymer by-products on the chemical properties of PEU polymer and the physical properties of PEU hydrogels. Removal of PEO-PPO diblock copolymers (P407_P) was found to preserve the thermo-responsiveness of resulting hydrogels, although slightly lower gelation onset temperature (T_{onset}) was found for P407_P (15.3°C) *vs*. P407 (16.7°C) hydrogels (25% w/V) as assessed through temperature ramp test. P407 and P407_P were then reacted with 1,6-diisocyanatohexane and 1,4-cyclohexanedimethanol to synthesize two different PEUs, coded as CHP407 and CHP407_P, respectively. Lower Number Average Molecular Weight ($\overline{M_n}$) and higher polydispersity Index (D) was measured for CHP407 ($\overline{M_n}$: 34 kDa, D: 1.6) respect to CHP407_P ($\overline{M_n}$: 40 kDa, D: 1.4) as a consequence of macrodiol purification. CHP407_P hydrogels formed bigger micelles (43.9 ± 4.1 nm *vs*. 28.7 ± 4 nm) while showed similar critical micellar temperatures (22.1°C *vs*. 21.6°C) respect to CHP407 formulations. Sol-to-gel transition of CHP407 and CHP407_P hydrogels was similar while CHP407_P gelation time at 37°C was longer as assessed by tube inverting test. The rheological analysis showed slightly lower T_{onset} for CHP407_P hydrogels (15% w/V), probably due to larger micelle size, promoting micellar assembly. However, CHP407_P hydrogels showed a significantly lower critical strain than CHP407 hydrogels, as assessed by strain sweep test, suggesting their higher brittleness due to a lower density of intermicellar bridge chains. Nano-scale hydrogel characterization by Low-Field Nuclear Magnetic Resonance spectroscopy supported previous findings, showing lower spin-spin relaxation time (i.e., 1,259 ms) for CHP407_P than for CHP407 hydrogels (i.e., 1,560 ms)

at 37°C, which suggested the formation of a more tightly packed network for CHP407_P than CHP407 hydrogel. Finally, lower swelling capability and resistance against dissolution were measured for CHP407_P hydrogels. Overall, the here-reported results suggested that the heterogeneous structure in the CHP407 hydrogel network caused by the presence of diblock copolymer-based macrodiols improved PEU hydrogel properties in light of their applicability in the biomedical field.

Keywords: poly(ether urethane)s, reagent purity, hydrogel performances, nanoscale characterization, micellar hydrogels, thermo-sensitive hydrogels

INTRODUCTION

Linear poly(urethane)s are known to be a versatile family of synthetic block-copolymers resulting from the reaction between three main building blocks, namely a macrodiol, a diisocyanate and a chain extender. The versatility of this class of polymers basically derives from their LEGO-like structure, which allows the synthesis of materials with different properties by simply changing their building blocks. Due to this unique feature, poly (urethane)s are widely used in extremely different fields, e.g., transportation, packaging, electronics and chemical and textile industries. Based on the selected reagents, the poly(urethane) family can be further subdivided into many sub-classes, such as thermoplastic, elastomeric, water-soluble and stimuli-responsive poly(urethane)s. For instance, thermoplastic poly (urethane)s have been usually synthesized using poly (ε-caprolactone), poly(lactic acid) or poly(hydroxyalcanoate)s as building blocks (Chen et al., 2013; Wang et al., 2019; Ping et al., 2005, Chen et al., 2003). On the other hand, water-soluble poly(urethane)s have been commonly designed by embedding poly(ethylene glycol) (PEG) moieties into their backbone (Caddeo et al., 2019; Doseva et al., 2004). Furthermore, through a proper selection of poly(ethylene glycol)-based building blocks, molecular weight and molar ratio, it is possible to synthesize amphiphilic water-soluble poly(urethane)s which aqueous solutions show a thermo-responsive behavior (Polo Fonseca et al., 2016; Ronco et al., 2017; Boffito et al., 2019). Among stimuli-responsive poly (urethane)s, different strategies have been explored to provide polymers with sensitivity to external stimuli. For instance, Boffito and colleagues (Boffito et al., 2020) synthesized a multi-functional poly(ether urethane) (PEU) by selecting an amphiphilic macrodiol (i.e., Poloxamer® 407) and a chain extender exposing primary amines (i.e., N-Boc Serinol) to ensure hydrogel thermo-sensitivity and acid pH-responsiveness, respectively. In another work, to provide poly (urethane)s with responsiveness to light irradiation, Pereira et al. (2010) reacted poly(ε-caprolactone) diol or poly (propylene glycol) with isophorone diisocyanate and 2-hydroxyethyl methacrylate, thus exposing photo-sensitive moieties. Differently, to the same final purpose, Laurano et al. (2020) selected an amino-group bearing chain extender (i.e., N-Boc diethanolamine) to first synthesize a high molecular weight poly(urethane), which was later functionalized with thioglycolic acid through carbodiimide-mediated reactions to expose thiol groups. Within each sub-class of poly(urethane)s, many works have been published on the investigation of the influence of reagent properties on the final polymer mechanical, biological and stability behaviors (Zhang et al., 2010; Ng et al., 1973; Tanaka and Kunimura, 2002; Gradinaru et al., 2012; Sartori et al., 2013; Silvestri et al., 2014; Mystkowska et al., 2017; Doseva et al., 2004, Lee et al., 2018). However, to the best of our knowledge, no works have been reported focusing on the relationship occurring between reagent purity and the resultant poly(urethane) properties and deriving performances. Poloxamers® are a family of commercial amphiphilic triblock copolymers extensively applied for the synthesis of PEUs forming hydrogels with improved thermo-sensitivity and stability in watery medium compared to Poloxamer®-based systems (Boffito et al., 2016; Cohn et al., 2006; Bonilla-Hernández et al., 2020; Whang et al., 2018; Lan et al., 1996). Within the Poloxamer® family, Poloxamer® 407 (P407) is a poly(ethylene oxide)-poly(propylene oxide)-poly(ethylene oxide) (PEO-PPO-PEO) triblock copolymer with 70% wt PEO content. However, P407 also contains PEO-PPO diblock copolymers resulting from the synthesis procedure and not completely removed during the purification steps. Therefore, P407 is characterized by a bimodal molecular weight distribution profile, with the low molecular weight component potentially affecting the physico-chemical properties of synthesized PEUs. In a recently published work, Fakhari et al. (2017) proposed a purification method able to reduce the PEO-PPO content, preserving hydrogel thermo-sensitivity and improving their mechanical behavior. Based on results on purified P407 and on a recently published method for the synthesis of a high molecular weight PEU containing P407 blocks (Laurano and Boffito 2020), this work was aimed at studying the properties of the PEU synthesized from P407, before and after its purification. Specifically, P407 was first subjected to the purification procedure (P407_P) proposed by Fakhari et al. (2017) and characterized to assess the repeatability of the published protocol. Subsequently, both P407 as such and P407_P were reacted with 1,6-hexamethylene diisocyanate and 1,4-cyclohexanedimethanol to obtain a high molecular weight PEU. The success of the synthesis was verified through infrared spectroscopy and chromatographic analyses. Subsequently, PEU chain capability to arrange into organized micelles upon dissolution in aqueous media was studied by estimating the micelle average hydrodynamic diameters and the critical micellar temperature (CMT). Then, hydrogel thermo-responsiveness and structural changes were studied both at the

macro-scale through rheological characterization, and at the nano-scale exploiting an innovative, non-destructive technique named Low-Field Nuclear Magnetic Resonance spectroscopy (LF-NMR) (Li et al., 2017). Lastly, hydrogel dissolution and swelling behavior in contact with simulated body fluids (i.e., Trizma® buffer, pH 7.4) was investigated, defining the most promising PEU formulation for biomedical applications.

MATERIALS AND METHODS

Poloxamer® 407 Purification

To remove impurities and by-product low molecular weight chains, i.e., diblock copolymers composed of poly(ethylene oxide)-poly(propylene oxide) (PEO-PPO), Poloxamer® 407 (P407, PEO-PPO-PEO triblock copolymer, $\overline{M_n}$ 12,600 Da, 70% wt PEO, Sigma-Aldrich, Italy) was subjected to a purification step according to the method reported by Fakhari et al. (2017) with slight modifications. More in detail, at each time point, the time required for a complete phase separation was reduced to 7 h (see **Supplementary Material** for a detailed description of the adopted protocol).

Hereafter, the purified macrodiol will be referred to with the acronym P407_P.

Purified Poloxamer® 407 Characterization

To assess the successful removal of low molecular weight chains and to verify the repeatability of the procedure, Size Exclusion Chromatography (SEC) and Attenuated Total Reflectance Fourier Transform Infrared (ATR-FTIR) spectroscopy were performed on P407_P samples belonging to three different purified batches. The same analyses were also performed on the commercial P407 for comparison. Furthermore, rheological characterization was conducted on P407_P hydrogels to investigate changes in hydrogel thermo-responsiveness with respect to P407 formulations.

Size Exclusion Chromatography

SEC analyses were performed through an Agilent Technologies 1,200 Series (CA, United States) equipped with a Refractive Index (RI) detector and two Waters Styragel columns (HR1 and HR4) conditioned at 55°C. N,N-dimethylformammide (DMF, CHROMASOLV Plus, inhibitor free, for HPLC, 99.9%, Carlo Erba Reagents, Italy), added with 0.1% w/V LiBr (Sigma-Aldrich, Italy), was used as mobile phase. A calibration curve based on poly(ethylene glycol) standards was defined in the range of peak molecular weight M_P 4,000–200,000 Da. Before analyses, 2 mg of polymer were dissolved in 1 ml of mobile phase and filtered through a 0.45 μm syringe filter (poly(tetrafluoroethylene) membrane, Whatman). Number Average Molecular Weight ($\overline{M_n}$), Weight Average Molecular Weight ($\overline{M_w}$) and polydispersity index (D) were estimated using the Agilent ChemStation software. The molecular weight distribution profiles were reported as average data of the three analyzed batches, while $\overline{M_n}$, $\overline{M_w}$ and D were reported as mean ± standard deviation.

Attenuated Total Reflectance Fourier Transform Infrared Spectroscopy

ATR-FTIR spectroscopy was conducted to verify the integrity of the characteristic P407 bonds and the absence of residual $(NH_4)_2SO_4$ salt content. Analyses were performed at room temperature (RT) using a Perkin Elmer spectrum 100 equipped with an ATR accessory (UATR KRSS) with diamond crystal. Spectra resulted from 32 scans in the range 4,000–600 cm^{-1} with a resolution of 4 cm^{-1}. Results were elaborated using the Perkin Elmer software and reported as average spectra.

Rheological Characterization

The rheological characterization was conducted using a stress-controlled rheometer (MCR302, Anton Paar Gmbh, Graz, Austria) equipped with a 50 mm parallel plate geometry and a Peltier system for temperature control. Samples were prepared by dissolving the polymer at 25% w/V concentration in double distilled water at 4°C overnight. Sol-to-gel transition was studied through temperature ramp tests carried out in the range 0–40°C, at 2°C/min rate and 0.1 s^{-1} frequency to avoid micelle disentanglement phenomena during the initial phase of the gelation process. On the other hand, strain sweep tests were conducted at 37°C (10 Hz, strain range 0.01–500% (Boffito et al., 2016)) to investigate gel resistance to applied deformation. Lastly, frequency sweep tests were performed within the linear viscoelastic region (frequency range 0.1–100 rad/s, strain 0.1%) at 25°C, 30°C and 37°C to characterize gel viscoelastic properties. For each analysis the sample was poured on the lower plate of the rheometer in the sol state at 0°C, heated at the test temperature and equilibrated for 10 min to reach thermal stability before testing.

Poly(ether urethane) Synthesis

Materials

PEUs were synthesized using either commercial P407 or P407_P as macrodiol, 1,4-cyclohexanedimethanol (CDM) as chain extender and 1,6-hexamethylene diisocyanate (HDI) as diisocyanate. CDM, HDI and dibutyltin dilaurate (DBTDL) were purchased from Sigma-Aldrich, Italy. Before use, reagents were properly treated to remove residual water and stabilizers (Pontremoli et al., 2018). Briefly, the macrodiol was dried under reduced pressure (approx. 200 mbar) at 100°C for 8 h and then cooled down to RT under vacuum; HDI was distilled under reduced pressure; CDM was stored at RT and under vacuum in a desiccator; 1,2-dichloroethane (DCE) was poured over activated molecular sieves (3 Å, activation at 120°C overnight, Sigma-Aldrich, Italy) and maintained overnight under nitrogen atmosphere. All solvents were purchased from Carlo Erba Reagents (Italy) in analytical grade.

Synthesis Protocol

PEU synthesis was carried out following the pre-polymerization method recently described by Boffito et al. (2019). Briefly, the

macrodiol (P407 or P407_P) was initially dissolved in anhydrous DCE (20% w/V concentration) at 80°C under stirring and continuous nitrogen flow. Subsequently, HDI was added at 2: 1 molar ratio with respect to the macrodiol and the pre-polymerization reaction proceeded for 150 min after the addition of a catalytic amount of DBTDL (0.1% w/w with respect to the macrodiol). At the end of the first step, the mixture was cooled down to 60°C and CDM (3% w/V in anhydrous DCE) was added to the isocyanate-terminated pre-polymer solution at unitary molar ratio respect to the macrodiol. This second step of the reaction was carried on for 90 min and finally terminated through the addition of anhydrous methanol. The polymer was finally collected by precipitation in petroleum ether (4:1 volume ratio with respect to DCE total volume). To remove the catalyst and residual by-products, the polymer was then dissolved in DCE (20% w/V) and purified through precipitation in a mixture of diethyl ether/methanol (98/2 V/V, 5:1 volume ratio with respect to DCE). Finally, the PEU was collected through centrifugation (Hettik, MIKRO 220R) at 0°C and 6,000 rpm for 20 min, dried overnight under the fume hood and stored at 4°C under nitrogen atmosphere until use.

Hereafter, the synthesized PEUs will be referred to with the acronyms CHP407 and CHP407_P, where C and H identify the chain extender and the diisocyanate, respectively, while P407 and P407_P refer to the macrodiol used for the synthesis.

Poly(ether urethane) Characterization

Size Exclusion Chromatography

To verify the successful synthesis of a high molecular weight polymer and to investigate the influence of macrodiol purity on the resultant PEU molecular weight distribution profile, SEC analysis was performed on both CHP407 and CHP407_P according to the method previously described for macrodiol characterization. The molecular weight distribution profiles were reported as average data of samples belonging to three different syntheses, while $\overline{M}_n$, $\overline{M}_w$ and D were reported as mean ± standard deviation.

Attenuated Total Reflectance Fourier Transform Infrared Spectroscopy

To assess the appearance of the characteristic vibrational bands of urethane bonds, ATR-FTIR spectroscopy was performed on both CHP407 and CHP407_P according to the protocol previously reported for macrodiol characterization. Analyses were performed in triplicate and results were reported as average spectra.

Dynamic Light Scattering

To investigate the relationship existing between PEU molecular weight distribution profile and micelle average hydrodynamic diameter, Dynamic Light Scattering (DLS) measurements were performed on both CHP407 and CHP407_P samples. To this aim, PEUs were dissolved at 0.5% w/V concentration in physiological saline solution (0.9% w/V NaCl). Analyses were performed at 25°C, 30°C, and 37°C, according to the protocol reported by Laurano et al. (2020), using a Zetasizer Nano S90 (Malvern Instruments, Worcestershire, United Kingdom) instrument. Before analysis, samples were equilibrated at the testing temperature for 15 min and then analyzed according to Pradal et al. (2013). The reported hydrodynamic diameters resulted from the average of three different analyzed samples. Data were reported as mean ± standard deviation.

Critical Micellar Temperature Evaluation

To investigate the effect of PEU molecular weight distribution profile on the temperature at which micelle nucleation begins, the CMT of PEU-based aqueous solutions was estimated using a fluorescent dye (1,6-diphenyl-1,3,5-hexatriene, DPH, Sigma-Aldrich, Italy) as micellization marker. Samples (1 ml) were prepared by dissolving the polymer at 0.5% w/V concentration in physiological saline solution (0.9% w/V NaCl). Then, DPH (0.4 mM in methanol) was added to each sample at 10 μl/ml. Analyses were conducted according to the method described by Alexandridis et al. (1994). Briefly, CHP407 and CHP407_P solutions were heated between 5°C and 40°C at 1°C/step, each step consisting of 5 min equilibration followed by UV/Vis spectra recording in the 500–300 nm spectral range (Perkin Elmer, Lambda 25). Finally, CMT was defined as the first inflection of the sigmoidal curve obtained by plotting the absorbance intensity at 356 nm *vs.* temperature as described by Boffito et al. (2016).

Poly(ether urethane)-Based Hydrogel Preparation

CHP407- and CHP407_P-based hydrogels were prepared in Bijou sample containers with an inner diameter of 17 mm (Carlo Erba Reagents, Italy) by dissolving the polymer at predefined concentrations (ranging between 5% w/V and 25% w/V) in physiological saline solution (0.9% w/V NaCl). To avoid micellization and/or gelation phenomena, which would prevent complete polymer dissolution, samples were kept at 4°C overnight.

Poly(ether urethane)-Based Hydrogel Characterization

Tube Inverting Test

Tube Inverting Test was performed to qualitatively determine the Critical Gelation Concentration (CGC) of CHP407- and CHP407_P-based solutions and to evaluate their sol-to-gel transition temperature. Specifically, samples (1 ml) were prepared as previously described and subjected to a controlled heating from 5°C to 70°C. Each step consisted of a 1 ± 0.1°C temperature increase within 30 s followed by temperature maintenance for 5 min and tube inversion that allowed the visual inspection of the sol-to-gel transition. Sol and gel conditions were defined as reported by Laurano and Boffito (2020). Briefly, "flow liquid sol" and "no flow solid gel" within 30 s of vial inversion identified the sol and gel states, respectively.

Gelation Time Test at Physiological Temperature

Gelation time test was performed at 37°C to estimate the time required by CHP407- and CHP407_P-based solutions to undergo sol-to-gel transition at physiological temperature. Specifically,

samples (1 ml) were prepared according to the above reported protocol and put in an incubator (Memmert IF75) equilibrated at 37°C. Then, at predefined time points (1–10 min, 1 min/step) samples were taken from the incubator and inverted for 30 s for the visual inspection of their sol/gel state. Conditions of sol and gel were defined as in the Tube Inverting Test. At each time point, the samples were equilibrated at 4°C for 8 min before incubation at 37°C to ensure that all systems were in the sol state at the beginning of the test.

Rheological Characterization

The influence of macrodiol purification on the capability of PEU aqueous solutions to undergo a sol-to-gel transition upon temperature increase was thoroughly investigated by means of rheological temperature ramp, frequency sweep and strain sweep tests. Specifically, CHP407 and CHP407_P samples were prepared by dissolving the polymer in physiological saline solution at the optimized concentration as defined in the Tube Inverting and Gelation Time tests. Then, both sol-gel systems were analyzed according to the protocol previously described for macrodiol rheological characterization.

Low Field Nuclear Magnetic Resonance Spectroscopy

To investigate whether the macrodiol molecular weight polydispersity could affect the PEU chain self-assembly capability into micelles in aqueous media, LF-NMR spectroscopy was exploited for an in depth nano-scale characterization. Specifically, analyses were performed on both CHP407 and CHP407_P systems using a Bruker Minispec mq20 (0.47T, Germany). The spin-spin relaxation times T_2 of PEU-based systems were measured according to the Carr-Purcell-Meiboom-Gill sequence with a 90°–180° pulse separation of 0.25 ms (number of scans = 4, delay = 5 s). To this aim, samples (500 μl at the optimized concentration) were prepared in NMR glass tubes (diameter 8 mm) and stored at 4°C until use. Then, they were incubated at 37 °C and the T_2 value was recorded at 0, 4, 8, and 10 min. Subsequently, the T_2 discrete distribution was obtained following the protocol published by Marizza et al. (2016).

Hydrogel Behavior in Aqueous Environment

Swelling and stability tests were carried out on CHP407_P hydrogels to evaluate if the absence of low molecular weight components into the macrodiol used for its synthesis could affect the stability of the systems in a watery environment. CHP407 hydrogels were also characterized for comparison. Samples (1 ml) were first prepared as previously described. Then, they were weighed to record their initial weight (W_i) and incubated at 37°C for 15 min to allow a complete sol-to-gel transition. Subsequently, 1 ml of Trizma® (0.1 M, pH 7.4, Sigma-Aldrich, Italy), previously equilibrated at 37°C to avoid gel destabilization, was added to each vial and samples were incubated for 6 h, 1, 2, 3, 7, and 14 days. Complete medium refresh was performed every other day. At each time step, three samples were taken, the residual medium was removed and the hydrogels were weighed (W_f) to assess their absorption ability (Apparent swelling %). Then, the samples were freeze-dried and weighed again ($W_{freeze\text{-}dried\_f}$) to quantify their weight loss (Weight loss %). Control samples (not incubated in Trizma® solutions) were also freeze-dried and weighed ($W_{freeze\text{-}dried\_i}$). Buffer absorption and system stability in aqueous environment were estimated according to the following equations:

$$Apparent\ swelling\ (\%) = \frac{W_f - W_i}{W_f} x\ 100 \quad (1)$$

$$Weight\ loss\ (\%) = \frac{W_{freeze-dried\_i} - W_{freeze-dried\_f}}{W_{freeze-dried\_i}} x\ 100 \quad (2)$$

Statistical Analysis

Statistical analysis was performed using GraphPad Prism 8.0 for MacOsX (GraphPad Software, La Jolla, CA, United States; www.graphpad.com). Two-way ANOVA analysis followed by Bonferroni's multiple comparison test was used to compare results. The statistical significance of each comparison was assessed as reported in (Boffito et al., 2016).

RESULTS AND DISCUSSION

Poloxamer® 407 is a commercial PEO-PPO-PEO triblock copolymer. However, it also contains PEO-PPO diblocks as by-products of the reaction synthesis. Therefore, P407 shows a bimodal molecular weight distribution profile (Fakhari et al., 2017). If it is exploited as starting reagent for the synthesis of a higher molecular weight polymer (e.g., PEUs), the presence of these by-products in the mixture may affect the resultant polymer properties. Therefore, in this work P407 was first subjected to a purification step (Fakhari et al., 2017) to remove the residual impurities and low molecular weight polymeric component (i.e., diblock copolymers). Then, the effects of P407 purification on the synthesis of a high molecular weight PEU as well as on the gelation mechanism and properties of PEU-based hydrogels were thoroughly investigated.

Poloxamer® 407 Physico-Chemical Characterization

Commercially available P407 was purified according to the protocol recently reported by Fakhari et al. (2017). The success and the repeatability of the treatment were verified through SEC and ATR-FTIR analyses, while changes in hydrogel thermo-sensitivity were assessed by means of rheological tests. Results on P407_P characterization were reported as **Supplementary Material**.

Poly(ether urethane) Chemical Characterization

To investigate whether the macrodiol purification could affect the success of poly(ether urethane) synthesis, ATR-FTIR spectroscopy was conducted on CHP407_P samples synthesized from three different batches of P407_P. The

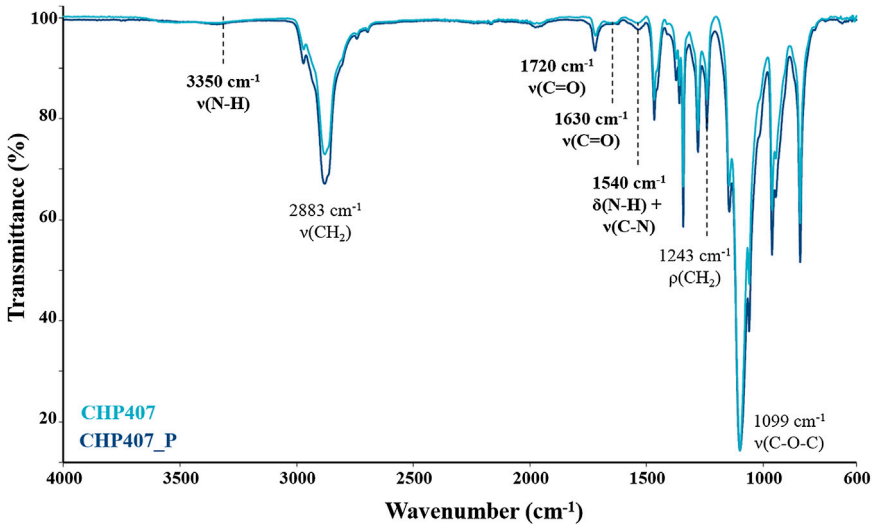

FIGURE 1 | Average ATR-FTIR spectra of CHP407 (light blue) and CHP407_P (dark blue) polymers. The bands proving the success of the synthesis are highlighted in bold.

average CHP407_P spectrum was then compared to that of CHP407 (**Figure 1**).

Irrespective of the macrodiol used, both spectra showed the characteristic bands ascribed to newly formed urethane bonds, thus proving the success of the synthesis. Specifically, the bands at 1,720 cm^{-1} and 1,630 cm^{-1} can be ascribed to the stretching vibration of carbonyl groups; the band at 3,350 cm^{-1} can be attributed to the stretching vibration of N-H bonds, while at 1,540 cm^{-1} the spectrum showed the bending vibration band of N-H bonds together with the stretching vibration band of C-N bonds (Laurano et al., 2019; Laurano et al., 2020).

Additionally, the Weight Average Molecular Weight ($\overline{M}_w$) and the Number Average Molecular Weight ($\overline{M}_n$) of the synthesized PEUs, measured through SEC analysis, were higher respect to that of the macrodiol, further confirming the synthesis of a high molecular weight polymer. Moreover, average CHP407_P molecular weights were slightly higher than for CHP407 (**Table 1**): the removal of PEO-PPO diblocks in the macrodiol avoids the formation of low molecular weight PEU chains (i.e., polymeric chains containing diblock instead of triblock macrodiol copolymers). Furthermore, the achievement of a more uniform molecular weight distribution was further proved by a reduction in the polydispersity index measured for CHP407_P PEU.

To deeply investigate changes in the molecular weight fractions in both polymers, contributing to the definition of such average values, the molecular weight distribution profiles of both CHP407 and CHP407_P were compared (**Figure 2**).

As reported in **Figure 2**, the maximum of the CHP407_P profile (M_i = 53,349 Da) was centered at values approx. equal to its $\overline{M}_w$ (i.e., 58,896 ± 1,160 Da), thus suggesting that the majority of CHP407_P chains were characterized by the same molecular weight. Conversely, the maximum of CHP407 profile was identified at 72,821 Da, hence significantly higher with respect to its $\overline{M}_w$ (i.e., 53,769 ± 1,365 Da). This result suggested the presence in CHP407 samples of a huge amount of low molecular weight chains, which lowered the Weight Average Molecular Weight. Indeed, while the lowest measured molecular weight for CHP407_P (M_i) was 10,550 Da, lower M_i values were registered for CHP407.

TABLE 1 | Number Average Molecular Weight ($\overline{M}_n$), Weight Average Molecular Weight ($\overline{M}_w$) and polydispersity index (D) estimated for CHP407 and CHP407_P polymers.

	Poly(ether urethane) parameters		
	$\overline{M}_n$ (Da)	$\overline{M}_w$ (Da)	D
CHP407	34,040 ± 1,290	53,769 ± 1,365	1.6 ± 0.03
CHP407_P	40,097 ± 980	58,896 ± 1,160	1.4 ± 0.02

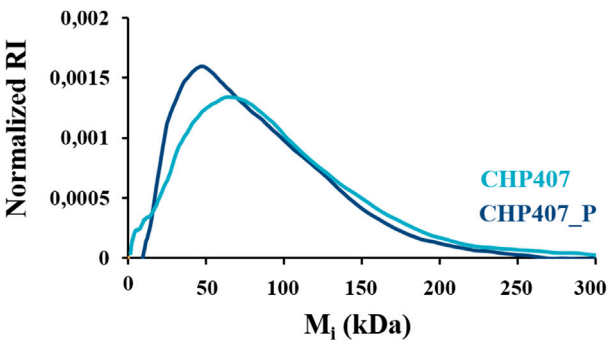

FIGURE 2 | Normalized Refractive Index (RI) signal as a function of molecular weight M_i measured for CHP407 (light blue spectrum) and CHP407_P (dark blue spectrum).

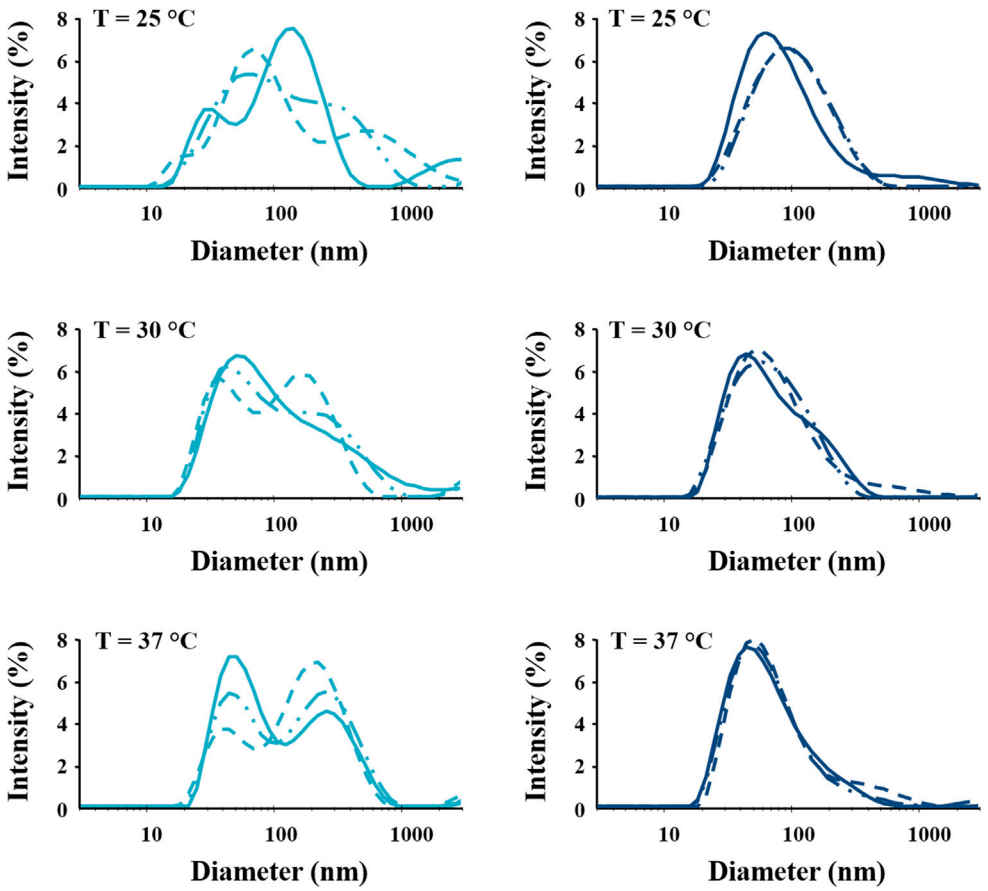

FIGURE 3 | Distribution patterns (by intensity) of micelle hydrodynamic diameter measured in CHP407 (light blue) and CHP407_P (dark blue) solutions at 0.5% w/V concentration. Analyses were performed in triplicate (continuous, dashed and dashed-dot lines represent the three registered patterns) at 25°C, 30°C and 37°C.

Thermo-sensitivity Evaluation of Poly(ether urethane)-Based Systems

CHP407 and CHP407_P chain capability to arrange into micelles upon temperature increase, derived from the presence of P407 or P407_P in their chains, was first investigated in not-gelling solutions through DLS measurements and by estimating their CMTs. Then, hydrogel thermo-sensitivity was definitely proved through Tube Inverting and Gelation Time tests, rheological characterization and Low Field Nuclear Magnetic Resonance spectroscopy. Lastly, hydrogel behavior in watery environment was investigated through swelling/stability tests.

Dynamic Light Scattering Measurements

DLS is a conventional technique usually applied to estimate the average hydrodynamic diameters of spherical structures, such as nanoparticles (Lim et al., 2013; Hoo et al., 2008). In this work, DLS measurements were adapted to investigate the effects of diblock removal from the macrodiol on the self-assembly capability of CHP407_P chains through the estimation of micelle hydrodynamic diameters. The same analyses were also performed on CHP407 for comparison. **Figures 3**, **4** report DLS intensity and volume patterns, respectively, measured at 25°C, 30°C, and 37°C for three different CHP407 and CHP407_P solutions.

As reported in **Figure 3** and **Table 2**, irrespective of the tested temperature, it was not possible to estimate a micelle average hydrodynamic diameter for CHP407 samples from the DLS intensity patterns, thus suggesting the simultaneous presence of both unimers and micelles, which continuously aggregate and disaggregate. Hence, the presence of a wide molecular weight polydispersity did not allow the formation of stable structures. Conversely, CHP407_P profiles turned out to be highly repeatable already at 25°C, with an average hydrodynamic diameter which can be attributed to micelles. These observations suggested the formation of more stable micelles as a consequence of the more uniform chain molecular weights.

For what concerns the distribution patterns by volume (**Figure 4**), both systems were able to give highly repeatable DLS measurements. Furthermore, despite the differences registered in the intensity patterns, both CHP407 and CHP407_P systems showed a unique hydrodynamic diameter distribution, which average value is characteristic of micelles (Boffito et al., 2016). However, at 25°C the average

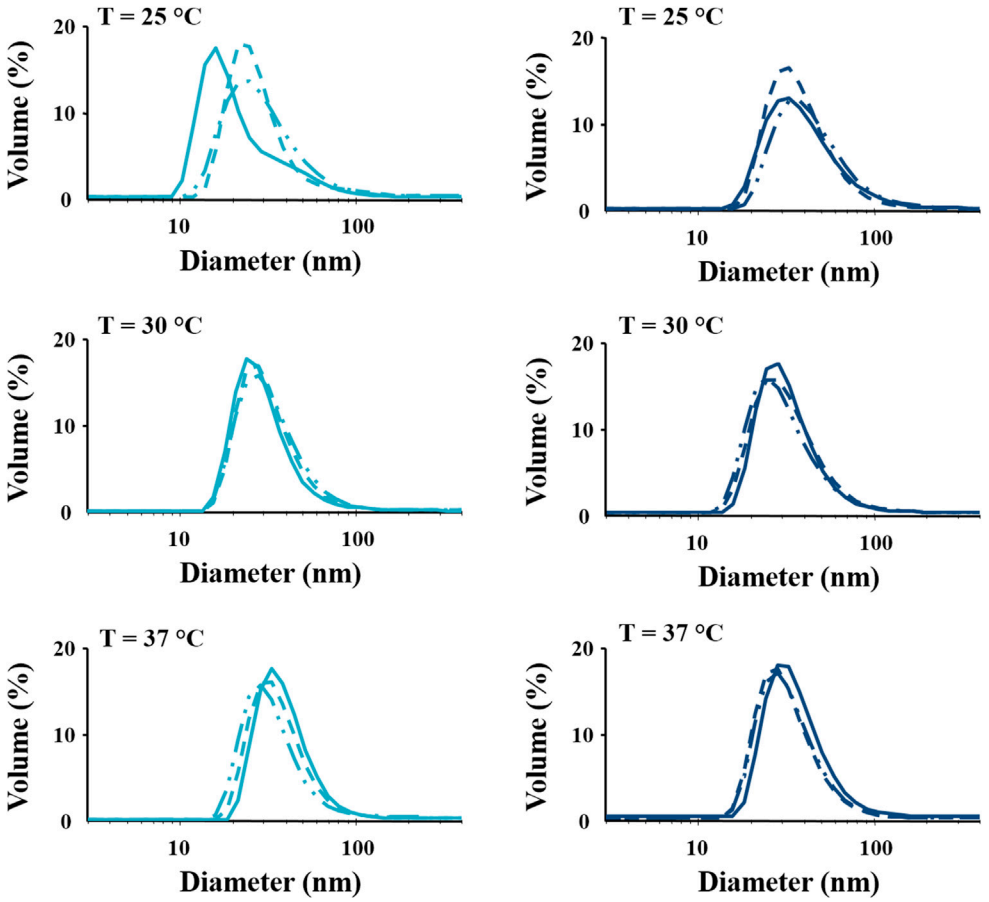

FIGURE 4 | Distribution patterns (by volume) of micelle hydrodynamic diameter measured in CHP407 (light blue) and CHP407_P (dark blue) solutions at 0.5% w/V concentration. Analyses were performed in triplicate (continuous, dashed and dashed-dotted lines represent the three registered patterns) at 25°C, 30°C and 37°C.

TABLE 2 | Micelle average hydrodynamic diameters by intensity and by volume measured for CHP407 and CHP407_P solutions (0.5% w/V concentration) at 25°C, 30°C, and 37°C.

	Micelle Hydrodynamic Diameter by Intensity (nm)		
	25°C	**30°C**	**37°C**
CHP407	-	-	-
CHP407_P	120.7 ± 15.4	82.2 ± 2.8	91.9 ± 1.8
	Micelle Hydrodynamic Diameter by Volume (nm)		
	25°C	**30°C**	**37°C**
CHP407	28.73 ± 4.02	34.60 ± 1.02	40.10 ± 1.42
CHP407_P	43.94 ± 4.13	35.25 ± 0.72	39.49 ± 1.78

hydrodynamic diameter of CHP407_P micelles turned out to be significantly higher with respect to CHP407 ones (**Table 2**). This evidence suggested that the absence of low molecular weight chains in CHP407_P led to the formation of bigger micelles at lower temperatures if compared to CHP407. On the other hand, further temperature increase leveled off this difference as comparable average hydrodynamic diameters were measured at 30°C and 37°C.

Estimation of the Critical Micellar Temperature

The CMT was estimated for both CHP407 and CHP407_P formulations to investigate whether the presence of a more uniform polymer molecular weight distribution could affect the temperature at which micelles begin to nucleate. To this aim, the fluorescent DPH dye was selected as micellization marker because it is almost non-fluorescent in water and gives a signal at 356 nm only when solubilized into the micelle hydrophobic core (**Figure 5**).

For both formulations, no DPH encapsulation was observed up to 20°C, suggesting the presence of polymeric chains in the form of unimers. At higher temperature, measured absorbance increased, with slightly higher values for CHP407 with respect to CHP407_P. These observations suggested the formation of a slightly higher amount of DPH-loaded CHP407 micelles, probably ascribed to an easier micelle nucleation process as a consequence of low molecular weight chains present within the system. This hypothesis was further supported by the estimated CMT value, which was measured to be slightly lower for CHP407 solution respect to

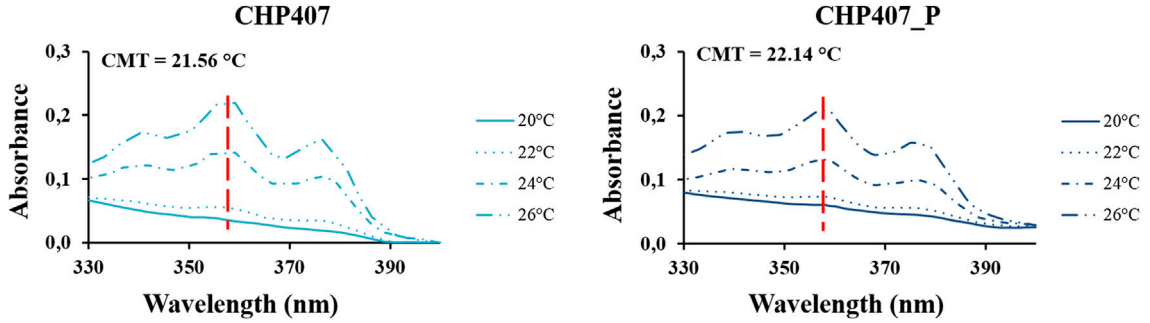

FIGURE 5 | UV/Vis spectra recorded in the 330–400 nm wavelength range for CHP407 and CHP407_P formulations (0.5% w/V concentration) upon temperature increase in the range 20°C–26°C. The red dashed lines mark the absorbance measured at 356 nm.

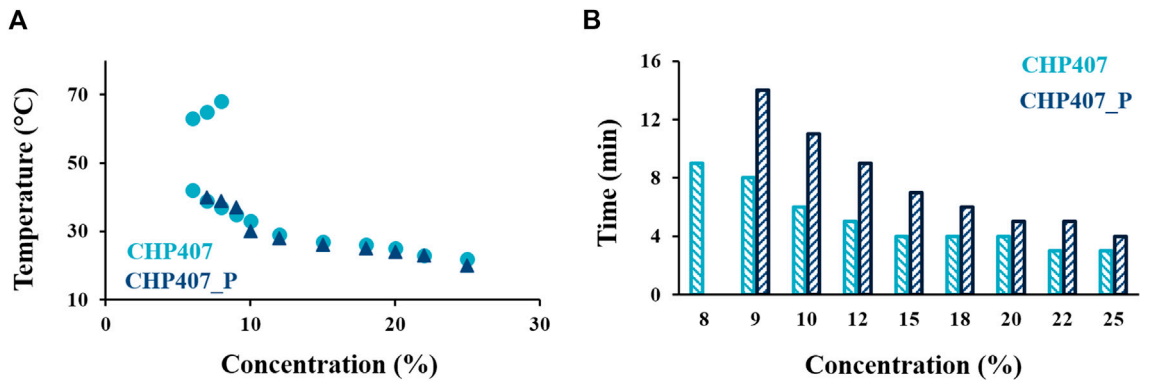

FIGURE 6 | Tube Inverting Test **(A)** conducted on CHP407 (light blue) and CHP407_P (dark blue) hydrogels (5%–25% w/V concentration range in physiological saline solution) within 5°C–70°C range (1°C/step, systematic error ±0.5°C). Gelation time test **(B)** at physiological temperature (1 min/step, systematic error ±30 s) performed on CHP407 (light blue) and CHP407_P (dark blue) hydrogels prepared by dissolving the polymer in physiological saline solution at different concentrations (5%–25% w/V).

CHP407_P one (i.e., 21.56°C *vs.* 22.14°C, respectively). Upon temperature increase up to 28°C, CHP407_P sample became turbid and thus, further absorbance measurements were not allowed. This evidence was probably attributed to the more uniform chain molecular weight distribution. Indeed, being the majority of the polymeric chains characterized by almost the same molecular weight, CHP407_P micelles most likely gave a more organized network, leading to higher crystallinity, which macroscopically resulted in a turbid solution.

Tube Inverting and Gelation Time Tests

Hydrogel capability to undergo a sol-to-gel transition in response to temperature increase was first qualitatively studied through the Tube Inverting test. Moreover, this test allowed also the definition of the CGC, i.e., the lowest polymer concentration able to form a solid gel. On the other hand, Gelation Time test conducted at 37°C gave information about hydrogel gelation timing in physiological-like conditions. As illustrated in **Figure 6A**, the gelation temperature of both CHP407 and CHP407_P hydrogels was strongly dependent on their polymeric concentration according to data reported in previous works on similar PEU-based systems (Boffito et al., 2016). Specifically, upon a decrease in polymer concentration a significant increase in the gelation temperature was observed, irrespective of the tested polymer. However, the CGC turned out to be slightly different for the two analyzed systems: 6% w/V and 7% w/V (error: ± 0.5% w/V) for CHP407 and CHP407_P gels, respectively. CHP407_P showed lightly lower gelation temperatures up to 10% w/V concentration and then slightly higher gelation temperature values from 10% w/V up to 7% w/V concentration compared to CHP407 systems. Furthermore, differently from CHP407 hydrogels, CHP407_P gels were not able to undergo a gel-to-sol transition upon further temperature increase (i.e., at temperatures higher than 60°C), further supporting the hypothesis on the formation of networks characterized by a higher crystallinity and thermal stability within a wider temperature range.

Concerning hydrogel gelation timing (**Figure 6B**), both systems showed a decrease in the time required to ensure a complete sol-to-gel transition at 37°C upon an increase in hydrogel concentration (Boffito et al., 2016). However, at each tested polymer concentration, CHP407_P hydrogels required more time to complete their gelation compared to CHP407

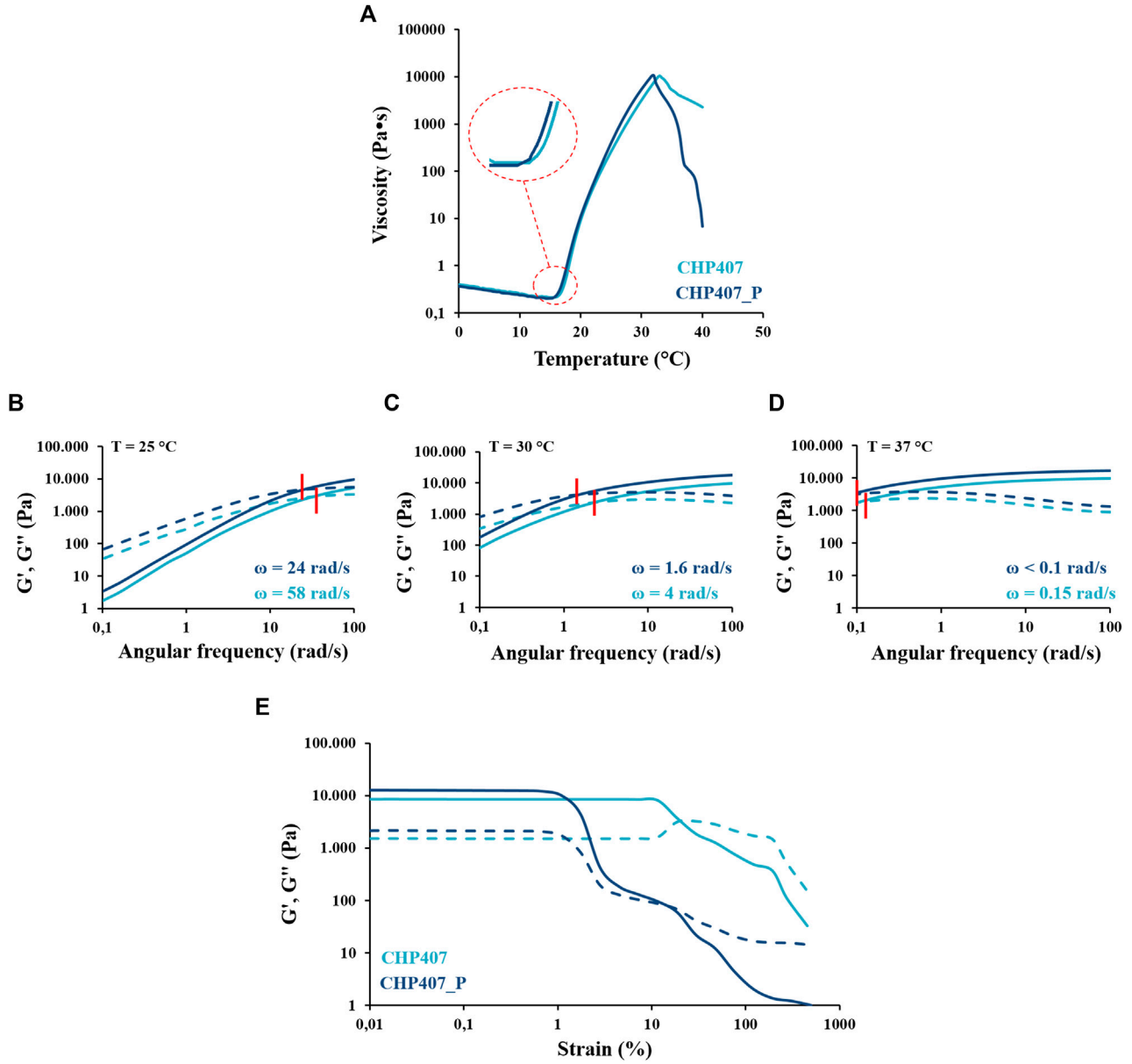

FIGURE 7 | (A) Viscosity profiles vs. temperature during sol-to-gel transition through temperature ramp test performed on CHP407 (light blue) and CHP407_P (dark blue) solutions (15% w/V concentration). **(B–D)** Frequency sweep test: storage (G'–continuous line) and loss (G"–dashed line) moduli registered for CHP407 (G', G"–light blue) and CHP407_P (G', G"–dark blue) gels at 25°C, 30°C, and 37°C. Red bars mark G'/G″ crossover point (ω). **(E)** Strain sweep test: storage (G'–continuous line) and loss (G"–dashed line) moduli registered as a function of applied deformation in the range 0.01%–500% for CHP407 (light blue) and CHP407_P (dark blue) sol-gel systems at 37°C.

formulations, as high molecular weight chains were not able to quickly arrange into a well-organized gel network, in agreement with findings on P407_P *vs.* P407 (see **Supplementary Material**). Nevertheless, despite these observations, the most promising hydrogel formulation able to undergo gelation at approx. physiological temperature within few minutes turned out to be the 15% w/V concentrated one for both CHP407 and CHP407_P gels. Indeed, these formulations showed a gelation temperature of 27°C and 26°C and a gelation time of 4 and 7 min for CHP407 and CHP407_P samples, respectively and thus, suitable for biomedical applications. Therefore, this composition was selected as the optimal one for the design of smart hydrogels and their further characterization.

Rheological Characterization

Rheological characterization was conducted on both CHP407_P and CHP407 sol-gel systems at the optimized concentration to thoroughly investigate changes in the temperature-driven gelation mechanism ascribable to their different molecular weight distribution and building block composition.

As proper of fluid behavior, the viscosity of both analyzed samples initially decreased as a function of temperature (**Figure 7A**), reaching a minimum value that was measured to be 0.3 Pa·s and 0.2 Pa·s for CHP407 and CHP407_P solutions, respectively. Although these values were very similar for both systems, in accordance with the slight differences in their average molecular weight values (**Table 1**), the gelation onset temperature (T_{onset}, defined at the minimum of viscosity) registered for CHP407_P hydrogel (i.e., 12.7°C) was slightly lower with respect to the CHP407 sample (i.e., 14.6°C). These data further supported DLS measurements (**Table 2**), which evidenced that CHP407_P formed bigger micelles at lower temperatures compared to CHP407 systems, favoring gelation start. Indeed, CHP407_P system was able to achieve the critical micellar volume required to begin the gelation process (Boffito et al., 2016) at slightly lower temperatures compared to CHP407 system. Differently, no differences were observed in micelle nucleation kinetics toward the achievement of the gel state upon further heating.

The process of gel formation and development upon temperature increase was studied through frequency sweep tests performed on both CHP407 and CHP407_P sol-gel systems (**Figures 7B–D**). Based on the conventionally defined relationship occurring between the storage (G') and the loss (G") moduli (Laurano and Boffito, 2020), both systems turned out to be mainly in the sol state at 25°C, in a biphasic phase at 30°C and not-completely developed gels at 37°C. The frequency at which G' becomes higher than G" ($\omega_{G'/G"\ crossover}$) is a peculiar parameter which marks the transition from viscous to elastic states. At each analyzed temperature, the crossover frequency of CHP407_P gels was measured to be lower respect to CHP407 (**Figures 7B–D**), suggesting the prevalent elastic behavior of CHP407_P formulation at each tested temperature.

Furthermore, at 37°C CHP407_P hydrogel was stronger compared to CHP407 hydrogel, as evidenced by the higher G'-G" delta (i.e., $\Delta_{G'-G"}$ = 10,468 and 6,894 Pa for CHP407_P and CHP407 hydrogels, respectively) measured at 0.01% deformation in strain sweep test (**Figure 7E**).

However, CHP407_P gels showed a significantly lower critical deformation (1.4%) compared to CHP407 sample (15.1%). This result suggested that the formation of a more organized network lowered hydrogel capability to resist against mechanical deformation. On the contrary, the presence in CHP407 formulations of chains characterized by different molecular weights favored the formation of "bridges" among micelles and thus, the establishment of an interconnected and more deformable network. The higher degree of organization and rigidity of CHP407_P network compared to CHP407 resulted in its drastic failure at low deformation. Differently, in CHP407 micro-cracks initially appeared within the gel network with G" increasing up to a maximum value, as typical of a strain hardening behavior. Upon G" reached a maximum value, macro-cracks appeared within the gel network leading to the complete failure of CHP407 gels with G" becoming higher than G', as typical of fluids.

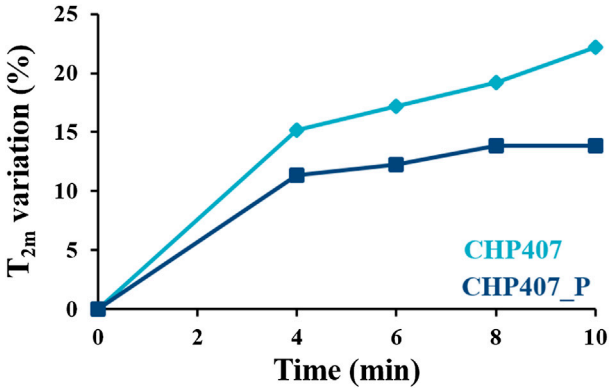

FIGURE 8 | Spin-spin relaxation time variation (%) respect to data measured at time zero as a function of time during temperature increase in the range 4°C–37°C for CHP407- and CHP407_P-based systems (light and dark blue, respectively).

Low Field Nuclear Magnetic Resonance Spectroscopy

To thoroughly investigate hydrogel structural changes occurring at the nano-scale in response to temperature increase, both CHP407 and CHP407_P samples were characterized exploiting the versatility of LF-NMR spectroscopy. This non-destructive technique provides information about water organization with respect to the surrounding polymeric chains by measuring the variation of water hydrogen spin-spin relaxation times (T_2) upon a very quick change in the orientation of an applied homogeneous magnetic field. Specifically, being permanent dipoles, water hydrogens are able to follow the direction of an applied magnetic field. Upon changes in magnetic field direction, changes in water hydrogen spin can be detected. The time water molecules require to recover their initial orientation, which is directly connected to T_2, depends on multiple parameters, such as temperature and polymeric chain spatial organization; thus, T_2 variations entail modifications in hydrogel structure. In the case of gels characterized by uniformity in the mesh size distribution, a unique relaxation time would exist. However, in a realistic polymeric system a poly-dispersed mesh size distribution occurs and thus, more than one relaxation time appear. In particular, each T_{2i} corresponds to a mesh class characterized by a specific size (ξ_i) (Abrami et al., 2018). The fraction of meshes characterized by the same T_{2i}/ξ_i is represented by the parameter A_i, so that the sum of all A_i is equal to 1. The weighed average of all the identified contributions defines the mean spin-spin relaxation time T_{2m}.

During sol-to-gel transition, T_{2m} generally decreases as a consequence of the reduced water mobility induced by the formation of the polymeric network upon temperature increase (Li et al., 2017; Malmierca et al., 2014). However, if the formation of the polymeric structure does not imply a clear increase in the fraction of the polymeric surface exposed to water molecules, the effect of temperature (which contributes to T_{2m} increase) cannot be negligible; consequently, T_{2m} can increase.

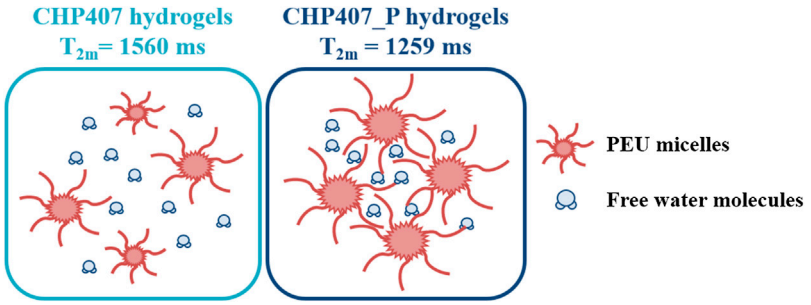

FIGURE 9 | Schematic representation of CHP407 and CHP407_P hydrogel internal structure at 37°C inspired by LF-NMR data.

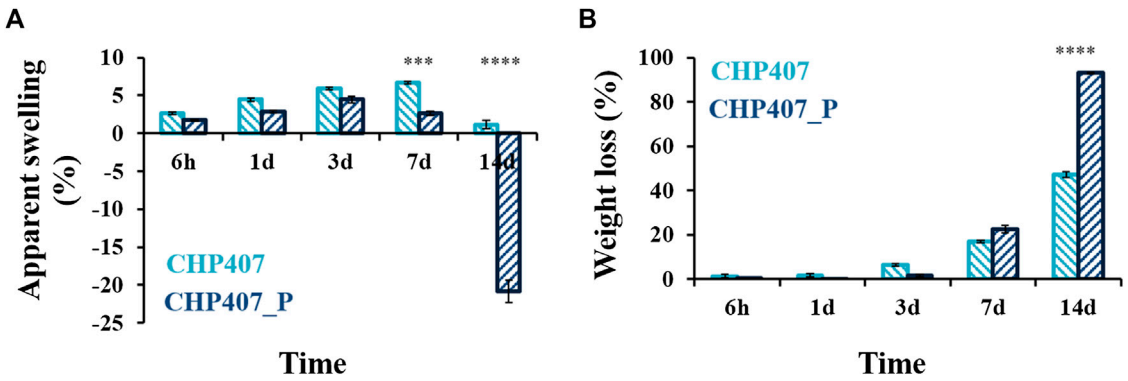

FIGURE 10 | Apparent swelling **(A)** and weight loss **(B)** percentages measured for CHP407 (light blue) and CHP407_P (dark blue) samples upon incubation in Trizma® buffer at 37°C for 6 h, 1, 3, 7, and 14 days. Data were reported as average values ± standard deviation.

In the presence of micellar gels, T_{2m} values are affected by both the formation of a network (decreasing water mobility and T_{2m}) and the effect of temperature increase (increasing T_{2m}) because micelle-based networks are not strong enough to make the temperature contribution negligible. Furthermore, during gel formation upon chain arrangement in the form of micelles, the polymeric superficial area interacting with water molecules reduces, resulting in a decrease of bound water and an increase of free water contribution.

Figure 8 reports the percentage variation (respect to data at time zero–see **Supplementary Table S1**) of T_{2m} as a function of time, for CHP407 and CHP407_P samples during temperature increase from 4 to 37°C. Hence, different time-points correspond to different temperatures. Data showed an increase of T_{2m} value for both CHP407 and CHP407_P systems over time, indicating a temperature dependence of this parameter.

At each time point, CHP407_P hydrogels showed lower T_{2m} values respect to CHP407. As both samples were subjected to the same heating ramp, differences in T_{2m} as a function of time were ascribed to differences in the hydrogel network structure. In CHP407 system, the presence of both high and low molecular weight chains allowed an initially faster micelle packing upon temperature increase (evidenced in **Figure 8** by higher T_{2m}–time curve slope of CHP407 compared to CHP407_P system). However, at 37°C CHP407 did not form a fully developed gel (in agreement with frequency sweep tests **Figures 7B–D**), as suggested by the increasing trend of T_{2m} values (no plateau value was achieved, suggesting that the process of gel formation was still in progress). On the contrary, gelation kinetics for CHP407_P formulation was initially slower but, once the micelle formed, their aggregation proceeded more rapid as a consequence of their uniform size, leading to a more stable and organized network at 37°C (suggested by the plateau value of T_{2m}) in agreement with rheological data.

Considering T_{2m} values at 10 min of analysis (i.e., systems in the gel state), CHP407-based gels showed a higher relaxation time compared to CHP407_P-based ones (i.e., 1,560 and 1,259 ms, respectively), reflecting a different internal structure pertaining to the two systems (**Figure 9**). This result can be attributed to the presence of polymeric chains characterized by different molecular weights. Indeed, the low molecular weight chains in CHP407 could act as blemishes during gel formation, thus leading, in the end, to a looser network. On the contrary, the narrower CHP407_P molecular weight distribution, as a consequence of P407 purification, resulted in tighter micelle packing, limiting

water molecules movements in the interstitial spaces among micelles.

Hydrogel Behavior in Aqueous Environment

In the perspective of hydrogel application in a physiological environment, swelling/stability tests were performed on CHP407 and CHP407_P systems in contact with simulated body fluids (i.e., Trizma® buffer, pH 7.4 at 37°C) at 37°C to evaluate the effects of macrodiol purification on the resultant poly (ether urethane) behavior in an aqueous environment (**Figure 10**).

Both systems showed similar fluid absorption capability and weight loss percentages up to 3 days of incubation. Conversely, a statistically significant difference was observed after 7 days of incubation, as CHP407 gels were able to absorb significantly higher amounts of external fluids (i.e., 6.7% *vs.* 2.7% for CHP407 and CHP407_P, respectively). At 14 days, negative apparent swelling percentages were registered for CHP407_P gels, thus suggesting that dissolution/erosion phenomena had completely overcome fluid absorption capability (i.e., CHP407_P gel dissolution achieved *ca.* 93% on day 14). Therefore, such results further supported the hypothesis formulated from LF-NMR data on a different nano-scale chain organization. Specifically, the removal of low molecular weight chains led to the formation of a highly organized network and, consequently, to detrimental effects on hydrogel stability over time. Indeed, in CHP407_P gels the presence of strongly packed micelles hindered the absorption of a considerable amount of fluids within the first days of incubation, but then, once water molecules started to infiltrate within the network, it underwent collapse due to its inability to resist deformation during swelling.

CONCLUSION

Poly(urethane)s are a class of synthetic polymers with *ad hoc* engineered structures, resulting from the accurate selection of the building blocks. Thus, poly(urethane)s show peculiar physico-chemical and mechanical features deriving from reagent properties and from their successful interactions. This work aimed at investigating the influence of macrodiol (i.e., Poloxamer® 407) molecular weight distribution on the resultant PEU polymer and hydrogel properties. To this aim, P407 was first subjected to a purification procedure to remove PEO-PPO diblock copolymers and impurities, while preserving its chemical structure (as assessed through ATR-FTIR spectroscopy). Then, SEC was exploited to verify the successful removal of by-products and the repeatability of the process. Moreover, purified P407 (i.e., P407_P) was also characterized in terms of thermo-responsiveness, showing slightly lower gelation onset temperatures (i.e., T_{onset} = 15.3°C *vs.* 16.7°C), faster gelation kinetics and slightly higher critical deformation (i.e., 3.5% *vs.* 2.3%) respect to not-purified P407 control sample. Subsequently, both P407 and P407_P macrodiols were exploited to synthesize CHP407 and CHP407_P, respectively, which turned out to show the same characteristic urethane vibrational bands, but different molecular weights and polydispersity indexes (i.e., $\overline{M}_n$ = 34 kDa *vs.* 40 kDa and D = 1.6 *vs.* 1.4 for CHP407 and CHP407_P, respectively). Moreover, the presence of a purified macrodiol in PEU chains also affected their capability to arrange into organized structures, giving more stable and bigger micelles for CHP407_P than for CHP407 systems (e.g., 43.94 ± 4.13 nm *vs.* 28.73 ± 4.02 nm).

Rheological temperature ramp tests showed that CHP407_P sol-gel systems were able to reach the critical micellar volume and thus, start their gelation process at lower temperatures compared to CHP407 ones (i.e., T_{onset} = 12.7°C *vs.* 14.6°C). Moreover, frequency sweep test data evidenced the prevalence of elastic behavior at increasingly lower frequencies for CHP407_P hydrogels respect to CHP407 at each analyzed temperature.

Additionally, rheological analysis also showed a considerably lower critical deformation (i.e. 1.4% *vs.* 15.1%) for CHP407_P, suggesting decreased deformability, attributed to the lack of micelle inter-bridges and the formation of a highly organized and rigid gel network.

These observations were further supported by an innovative analysis technique, i.e., the Low-Field Nuclear Magnetic Resonance spectroscopy, which allowed the nano-scale investigation of hydrogel network arrangement. Results confirmed the formation of a more organized structure, with a more packed network in the case of CHP407_P, resulting in limitations in water molecule mobility in the interstitial spaces among micelles.

However, the improved micelle packing by CHP407_P together with the lack of micelle inter-bridges caused a remarkable reduction of hydrogel stability in watery environment with almost complete dissolution/erosion of CHP407_P after 14 days of incubation.

Overall the results evidenced the influence of the purity of the starting P407 macrodiol on final PEU properties. In detail, a PEU with a narrower molecular weight distribution was synthesized from the purified macrodiol, after the removal of PEO-PPO diblock copolymers. In CHP407_P hydrogel, thermo-responsiveness was demonstrated involving the initial aggregation of significantly larger micelles than for CHP407 hydrogel. For this reason, the sol-to-gel transition of CHP407_P hydrogel began at slightly lower temperature (i.e., the critical volume required for the onset of gelation was achieved at lower temperature) and then proceeded with slightly faster kinetics, as suggested by frequency sweep tests. Due to their more regular structure with tightly packed homogeneous micelles, CHP407_P hydrogels showed reduced apparent swelling degree compared to CHP407 hydrogels. However, CHP407_P hydrogels were supposed to have a decreased density of inter-bridges among micelles, as they are generally formed by lower molecular weight chains. Hence, the decreased number of inter-bridges among micelles in CHP407_P hydrogels was probably the cause of their lower resistance to deformation and faster dissolution/erosion in aqueous medium. On the contrary, CHP407 hydrogels showed improved swelling capability and the ability to sustain higher deformations, attributed to the higher density of inter-bridges among micelles. In conclusion, the removal of

low molecular weight chains was detrimental for the performance of thermo-sensitive PEU hydrogels in the perspective of their future application in the field of drug delivery, or as bio-inks for bioprinting. Overall results could pave the way to the preparation of PEU thermo-sensitive hydrogels with superior mechanical properties and stability in physiological conditions, making use of amphiphilic macrodiols with different block structure (e.g., mixture of di-block and triblock copolymers).

DATA AVAILABILITY STATEMENT

All datasets presented in this study are included in the article/ **Supplementary Material**.

AUTHOR CONTRIBUTIONS

RL designed the experiments, performed the analyses, analyzed the data and wrote the paper; MA and MG performed the LF-NMR analyses; GC, MB and VC designed the experiments and provided scientific and financial support to the work. All authors reviewed the draft.

FUNDING

This project has received funding from the European Union's Horizon 2020 research and innovation program under grant agreement No. 685872-MOZART (www.mozartproject.eu) and from the European Research Council (ERC) under the European Union's Horizon 2020 research and innovation programme grant agreement No. 772168 (www.biorecar.polito.it).

SUPPLEMENTARY MATERIAL

The Supplementary Material for this article can be found online at: https://www.frontiersin.org/articles/10.3389/fmats.2020.594515/full#supplementary-material

REFERENCES

Abrami, M., Chiarappa, G., Farra, R., Grassi, G., Marizza, P., and Grassi, M. (2018). Use of low-field NMR for the characterization of gels and biological tissues. *Admet Dmpk.* 6, 34–46. doi:10.5599/admet.6.1.430

Alexandridis, P., Holzwarth, J. F., and Hatton, T. A. (1994). Micellization of poly(ethylene oxide)-poly(propylene oxide)-poly(ethylene oxide) triblock copolymers in aqueous solutions: thermodynamics of copolymer association. *Macromolecules* 27, 2414–2425. doi:10.1021/ma00087a009

Boffito, M., Gioffredi, E., Chiono, V., Calzone, S., Ranzato, E., Martinotti, S., et al. (2016). Novel polyurethane-based thermosensitive hydrogels as drug release and tissue engineering platforms: design and *in vitro* characterization. *Polym. Int.* 65, 756–769. doi:10.1002/pi.5080

Boffito, M., Pontremoli, C., Fiorilli, S., Laurano, R., Ciardelli, G., and Vitale-Brovarone, C. (2019). Injectable thermosensitive formulation based on polyurethane hydrogel/mesoporous glasses for sustained co-delivery of functional ions and drugs. *Pharmaceutics* 11, 501–521. doi:10.3390/pharmaceutics11100501

Boffito, M., Torchio, A., Tonda-Turo, C., Laurano, R., Gisbert Garzaran, M., Berkmann, J. C., et al. (2020). Hybrid injectable sol-gel systems based on thermo-sensitive polyurethane hydrogels carrying pH-sensitive mesoporous silica nanoparticles for the controlled and triggered release of therapeutic agents. *Front. Bioeng. Biotechnol.* 8, 384–408. doi:10.3389/fbioe.2020.00384

Bonilla-Hernández, M., Zapata-Catzin, G. A., de Jesús Castillo-Cruz, O., Vargas-Coronado, R. F., Cervantes-Uc, J. M., Xool-Tamayo, J. F., et al. (2020). Synthesis and characterization of metformin-pluronic based polyurethanes for controlled drug delivery. *Int. J. Polym. Mater.* 1. doi:10.1080/00914037.2020.1740996

Caddeo, S., Mattioli-Belmonte, M., Cassino, C., Barbani, N., Dicarlo, M., Gentile, P., et al. (2019). Newly-designed collagen/polyurethane bioartificial blend as coating on bioactive glass-ceramics for bone tissue engineering applications. *Mater. Sci. Eng. C* 96, 218–233. doi:10.1016/j.msec.2018.11.012

Chen, F.-T., Duo, Y.-Q., Luo, S.-G., Luo, Y.-J., and Tan, H.-M. (2003). Novel segmented thermoplastic polyurethanes elastomers based on tetrahydrofuran ethylene oxide copolyethers as high energetic propellant binders. *Propellants, Explos. Pyrotech.* 28, 7–11. doi:10.1002/prep.200390007

Chen, S.-H., Tsao, C.-T., Chou, H.-C., Chang, C.-H., Hsu, C.-T., Chuang, C.-N., et al. (2013). Synthesis of poly(lactic acid)-based polyurethanes. *Polym. Int.* 62, 1159–1168. doi:10.1002/pi.4400

Cohn, D., Lando, G., Sosnik, A., Garty, S., and Levi, A. (2006). PEO-PPO-PEO-based poly(ether ester urethane)s as degradable reverse thermo-responsive multiblock copolymers. *Biomaterials* 27, 1718–1727. doi:10.1016/j.biomaterials.2005.10.035

Doseva, V., Shenkov, S., Valisey, S., and Baranovsky, V. Y. (2004). Synthesis and properties of water soluble polyurethanes based on poly(ethylene glycol). *J. Appl. Polym. Sci.* 91, 3651–3658. doi:10.1002/app.13604

Fakhari, A., Corcoran, M., and Schwarz, A. (2017). Thermogelling properties of purified poloxamer 407. *Heliyon* 3, 1–26. doi:10.1016/j.heliyon.2017.e00390

Gradinaru, L. M., Ciobanu, C., Vlad, S., Bercea, M., and Popa, M. (2012). Thermoreversible poly(isopropyl lactate diol)-based polyurethane hydrogels: effect of isocyanate on some physical properties. *Ind. Eng. Chem. Res.* 51, 12344–12354. doi:10.1021/ie301690e

Hoo, C. M., Starostin, N., West, P., and Mecrtney, M. L. (2008). A comparison of atomic force microscopy (AFM) and dynamic light scattering (DLS) methods to characterize nanoparticle size distributions. *J. Nanopart. Res.* 10, 89–96. doi:10.1007/s11051-008-9435-7

Lan, P., Corneillie, S., Schacht, E., Davies, M., and Shard, A. (1996). Synthesis and characterization of segmented polyurethanes based on amphiphilic polyether diols. *Biomaterials* 17, 2273–2280. doi:10.1016/0142-9612(96)00056-7

Laurano, R., and Boffito, M. (2020). Thermosensitive micellar hydrogels as vehicles to deliver drugs with different wettability. *Front. Bioeng. Biotechnol.* 8, 708. doi:10.3389/fbioe.2020.00708

Laurano, R., Boffito, M., Torchio, A., Cassino, C., Chiono, V., and Ciardelli, G. (2019). Plasma treatment of polymer powder as an effective tool to functionalize polymers: case study application on an amphiphilic polyurethane. *Polymers* 11, 2109. doi:10.3390/polym11122109

Laurano, R., Cassino, C., Ciardelli, G., Chiono, V., and Boffito, M. (2020). Polyurethane-based thiomers: a new multifunctional copolymer platform for biomedical applications. *React. Funct. Polym.* 146, 104413. doi:10.1016/j.reactfunctpolym.2019.104413

Lee, S. Y., Wu, S. C., Chen, H., Tsai, L. L., Tzeng, J. J., Lin, C. H., et al. (2018). Synthesis and characterization of polycaprolactone-based polyurethanes for the fabrication of elastic guided bone regeneration membrane. *BioMed Res. Int.* 2018, 3240571. doi:10.1155/2018/3240571

Li, Y., Li, X., Chen, C., Zhao, D., Su, Z., Ma, G., et al. (2017). Sol-gel transition characterization of thermosensitive hydrogels based on water mobility variation provided by low field NMR. *J. Polym. Res.* 25, 1–10. doi:10.1007/s10965-017-1185-8

Lim, J., Yeap, S. P., Che, H. X., and Low, S. C. (2013). Characterization of magnetic nanoparticle by dynamic light scattering. *Nanoscale Res. Letters.* 8, 381–395. doi:10.1186/1556-276x-8-381

Malmierca, M. A., González-Jiménez, A., Mora-Barrantes, I., Posadas, P., Rodríguez, A., Ibarra, L., et al. (2014). Characterization of network structure and chain dynamics of elastomeric ionomers by means of ^{1}H Low-Field NMR. *Macromolecules* 47, 5665–5667. doi:10.1021/ma501208g

Marizza, P., Abrami, M., Keller, S. S., Posocco, P., Laurini, E., Goswami, K., et al. (2016). Synthesis and characterization of UV photocrosslinkable hydrogels with poly(N-vinyl-2-pyrrolidone): determination of the network mesh size distribution. *Int. J. Polym. Mater.* 65, 516–525. doi:10.1080/00914037.2015.1129964

Mystkowska, J., Mazurek-Budzyńska, M., Piktel, E., Niemirowicz, K., Karalus, W., Deptuła, P., et al. (2017). Assessment of aliphatic poly(ester-carbonate-urea-urethane)s potential as materials for biomedical application. *J. Polym. Res.* 24, 144. doi:10.1007/s10965-017-1296-2

Ng, H. N., Allegrezza, A. E., Seymour, R. W., and Cooper, S. L. (1973). Effect of segment size and polydispersity on the properties of polyurethane block polymers. *Polymer* 14, 255–261. doi:10.1016/0032-3861(73)90085-2

Pereira, I.H.L., Ayres, E., Patrício, P.S., Góes, A.M., Gomide, V.S., Junior, E.P., et al. (2010). Photopolymerizable and injectable polyurethanes for biomedical applications: synthesis and biocompatibility. *Act. Biomater.* 6, 3056–3066. doi:10.1016/j.actbio.2010.02.036

Ping, P., Wang, W., Chen, X., and Jing, X. (2005). Poly(ε-caprolactone) polyurethane and its shape-memory property†. *Biomacromolecules* 6, 587–592. doi:10.1021/bm049477j

Polo Fonseca, L., Bergamo Trinca, R., and Felisberti, M. I. (2016). Thermo-responsive polyurethane hydrogels based on poly(ethylene glycol) and poly(caprolactone): physico-chemical and mechanical properties. *J. Appl. Polym. Sci.* 133 (25), 43573–43583. doi:10.1002/app.43573

Pontremoli, C., Boffito, M., Fiorilli, S., Laurano, R., Torchio, A., Bari, A., et al. (2018). Hybrid injectable platforms for the *in situ* delivery of therapeutic ions from mesoporous glasses. *Chem. Eng. J.* 340, 103–113. doi:10.1016/j.cej.2018.01.073

Pradal, C., Jack, K. S., Grøndahl, L., and Cooper-White., J. J. (2013). Gelation kinetics and viscoelastic properties of pluronic and α-cyclodextrin-based pseudopolyrotaxane hydrogels. *Biomacromolecules* 14, 3780–3792. doi:10.1021/bm401168h

Ronco, L. I., Basterretxea, A., Mantione, D., Aguirresarobe, R. H., Minari, R. J., Gugliotta, L. M., et al. (2017). Temperature responsive PEG-based polyurethanes "à la carte". *Polymer* 122, 117–124. doi:10.1016/j.polymer.2017.06.043

Sartori, S., Boffito, M., Serafini, P., Caporale, A., Silvestri, A., Bernardi, E., et al. (2013). Synthesis and structure-property relationship of polyester-urethanes and their evaluation for the regeneration of contractile tissues. *React. Funct. Polym.* 73, 1366–1376. doi:10.1016/j.reactfunctpolym.2013.01.006

Silvestri, A., Sartori, S., Boffito, M., Mattu, C., Di Rienzo, A. M., Boccafoschi, F., et al. (2014). Biomimetic myocardial patches fabricated with poly(ε-caprolactone) and polyethylene glycol-based polyurethanes. *J. Biomed. Mater. Res.* 102, 1002–1013. doi:10.1002/jbm.b.33081

Tanaka, H., and Kunimura, M. (2002). Mechanical properties of thermoplastic polyurethanes containing aliphatic polycarbonate soft segments with different chemical structures. *Polym. Eng. Sci.* 42, 1333–1349. doi:10.1002/pen.11035

Wang, C., Wang, H., Zou, F., Chen, S., and Wang, Y. (2019). Development of polyhydroxyalkanoate-based polyurethane with water-thermal response shape-memory behavior as new 3d elastomers scaffolds. *Polymers* 11, 1030. doi:10.3390/polym11061030

Whang, C.-H., Lee, H. K., Kundu, S., Murthy, S. N., and Jo, S. (2018). Pluronic-based dual-stimuli sensitive polymers capable of thermal gelation and pH-dependent degradation for *in situ* biomedical application. *J. Appl. Polym. Sci.* 135, 46552. doi:10.1002/app.46552

Zhang, T., Wu, W., Wang, X., and Mu, Y. (2010). Effect of average functionality on properties of UV-curable waterborne polyurethane-acrylate. *Prog. Org. Coating.* 68, 201–207. doi:10.1016/j.porgcoat.2010.02.004

Conflict of Interest: The authors declare that the research was conducted in the absence of any commercial or financial relationships that could be construed as a potential conflict of interest.